

University of Nebraska - Lincoln

DigitalCommons@University of Nebraska - Lincoln

Faculty Publications from the Department of
Electrical and Computer Engineering

Electrical & Computer Engineering, Department of

12-1-1989

Ellipsometric study of $\text{Al}_2\text{O}_3/\text{Ag}/\text{Si}$ and $\text{SiO}_2/\text{Ag}/\text{quartz}$ ashed in an oxygen plasma

Bhola N. De

University of Nebraska-Lincoln

John A. Woollam

University of Nebraska-Lincoln, jwoollam1@unl.edu

Follow this and additional works at: <http://digitalcommons.unl.edu/electricalengineeringfacpub>



Part of the [Electrical and Computer Engineering Commons](#)

De, Bhola N. and Woollam, John A., "Ellipsometric study of $\text{Al}_2\text{O}_3/\text{Ag}/\text{Si}$ and $\text{SiO}_2/\text{Ag}/\text{quartz}$ ashed in an oxygen plasma" (1989).
Faculty Publications from the Department of Electrical and Computer Engineering. 51.
<http://digitalcommons.unl.edu/electricalengineeringfacpub/51>

This Article is brought to you for free and open access by the Electrical & Computer Engineering, Department of at DigitalCommons@University of Nebraska - Lincoln. It has been accepted for inclusion in Faculty Publications from the Department of Electrical and Computer Engineering by an authorized administrator of DigitalCommons@University of Nebraska - Lincoln.

Ellipsometric study of $\text{Al}_2\text{O}_3/\text{Ag}/\text{Si}$ and $\text{SiO}_2/\text{Ag}/\text{quartz}$ ashed in an oxygen plasma

Bhola N. De and John A. Woollam

Center for Microelectronic and Optical Materials Research, and Department of Electrical Engineering, University of Nebraska, Lincoln, Nebraska 68588-0511

Abstract

Using monolayer-sensitive variable angle of incidence spectroscopic ellipsometry, the silver oxide growth on a silver mirror, coated with an Al_2O_3 or SiO_2 protective layer, was investigated. The oxidation was done in a pure oxygen plasma asher. The resulting silver oxide growth was monitored accurately as a function of exposure time in the plasma asher. It was found that silver was converted to silver oxide under the protective coating, during ashing of a sample. The optical constants of a dense silver oxide thin film, created by oxidizing in the asher, were also measured.

Journal of Applied Physics is copyrighted by The American Institute of Physics.

DOI: 10.1063/1.343665

Permalink: <http://link.aip.org/link/?JAPIAU/66/5602/1>

Ellipsometric study of $\text{Al}_2\text{O}_3/\text{Ag}/\text{Si}$ and $\text{SiO}_2/\text{Ag}/\text{quartz}$ ashed in an oxygen plasma^{a)}

Bhola N. De and John A. Woollam

Center for Microelectronic and Optical Materials Research and Department of Electrical Engineering, University of Nebraska, Lincoln, Nebraska 68588-0511

(Received 13 July 1989; accepted for publication 9 August 1989)

Using monolayer-sensitive variable angle of incidence spectroscopic ellipsometry, the silver oxide growth on a silver mirror, coated with an Al_2O_3 or SiO_2 protective layer, was investigated. The oxidation was done in a pure oxygen plasma asher. The resulting silver oxide growth was monitored accurately as a function of exposure time in the plasma asher. It was found that silver was converted to silver oxide under the protective coating, during ashing of a sample. The optical constants of a dense silver oxide thin film, created by oxidizing in the asher, were also measured.

I. INTRODUCTION

The degradation of many materials, for example, silver mirrors, for use in a low-earth orbit space environment has recently drawn considerable attention. Various people are trying to engineer a proper protective coating to prevent oxidation and damage of the underlying sensitive material surfaces.¹⁻¹³ The low-earth orbit space environment roughly extends over the altitude range of 200–700 km. At these altitudes, there is an abundance of neutral ground-state atomic oxygen. As a result of the mean free path between collisions being very large, low-earth orbit altitudes provide a very long lifetime for atomic oxygen and various other species. One of the ways of forming atomic oxygen in low-earth orbit altitudes is the absorption of UV rays from the sun by molecular oxygen, which is thereby dissociated to form atomic oxygen.⁷ Atomic oxygen can also be formed through electron capture by molecular oxygen, followed by dissociation of this highly unstable anionic molecular complex to atomic oxygen and O^- . Moreover, these oxygen atoms have approximately 5 eV of ram impact kinetic energy on a moving space shuttle (velocity about 10 km/s). (For details on the distribution of the number density of various atoms and molecules as a function of altitude and other related information, see Ref. 1.)

One appropriate class of materials proposed for use as protective coatings is oxides.² If various space materials can be coated with an appropriately designed thin protective oxide layer, possibly having an amorphous structure, low defect density, and high activation energy for atomic oxygen diffusion, then long term survivability of various space-bound structures could be ensured. The thermal expansion and the adhesion between the film material and the substrate need to be appropriately adjusted so that microcracks are not formed inside the film because of thermal stress; this would otherwise form short circuit diffusion paths for atomic oxygen through the film, that could readily degrade the protected space material underneath the layer.

In this paper, a set of experiments regarding the penetration of atomic oxygen through an amorphous Al_2O_3 , or

SiO_2 overcoating, resulting in the growth of silver oxide film on top of silver has been described. The samples were exposed to a pure oxygen plasma in a plasma asher for a series of times using variable angle spectroscopic ellipsometry (VASE). VASE is well known to be a monolayer-sensitive, nondestructive technique used to study various material surfaces.¹⁴⁻²⁰

In order to properly perform VASE data analysis, the optical constants of silver oxide were needed. No reliable data on the optical constants of silver oxide, corresponding to that formed by the reaction of a high-quality silver film with the atomic oxygen, could be found in the literature. [Only one paper (Ref. 21) could be found, and it was for bulk silver oxide prepared by isostatically compressing silver oxide powder and mechanically polishing one side. It was most likely different, both in morphology and chemical constitution, from the silver oxide formed in the plasma asher.] Therefore, the optical constants of silver oxide, formed by ashing a high-quality silver film (evaporated onto a polished silicon wafer) in the oxygen plasma, were first experimentally determined. The optical constants of silver oxide were then used to model the growth of silver oxide films underneath the protective aluminum oxide or the silicon oxide layer.

This paper is organized as follows: in Sec. II, the asher used for oxidizing the samples is described; in Sec. III, a brief introduction is given to the principles of the VASE experiment and data analysis. In Sec. IV, the results of analysis of VASE data are described. Section V summarizes and concludes.

II. CHARACTERIZATION OF THE ASHER

An SPI Plasma Prep II asher (SPI Corporation) was used to expose the samples to an oxygen plasma, using high-purity oxygen. This had a capacitively coupled barrel-type plasma chamber, driven by a 13.6-MHz 100-W rf power source. Pure oxygen gas was introduced to the plasma chamber to generate the oxygen plasma, and the main chamber pressure was kept at 100 μm . An oxygen plasma is known to have various species such as $\text{O}(^3\text{P})$, O^- , O^+ , O_2^+ , O_2^- , $\text{O}_2(^1\Delta_g)$.³ To investigate the properties of the oxygen plasma in the asher, a barrel-type Pyrex glass tube asher was

^{a)} Research supported by NASA Lewis Research Center Grant No. NAG-3-95.

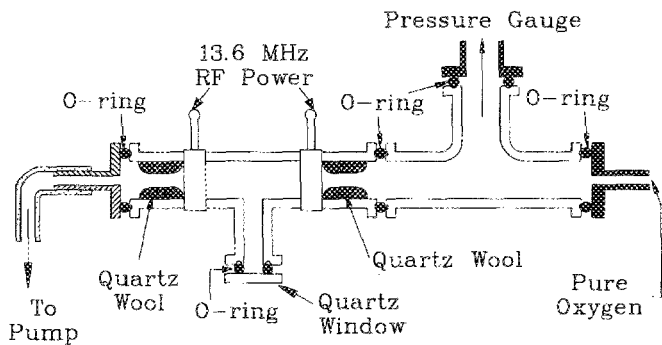


FIG. 1. Pyrex glass tube asher constructed to investigate the spectroscopic lines emanating from the oxygen plasma.

constructed, as shown in Fig. 1. Rolls of quartz wool with 1-cm-diam holes at the center prevented the plasma from coming in contact with various Viton O rings, used for joining various glass parts of the chamber. The quartz window was needed to receive the UV and visible emission lines from the plasma to a spectrum analyzer. The wavelengths of lines obtained from the oxygen plasma and their identifications are shown in Table I. The relative intensities of various lines could not be obtained with any reliability because of noise from the rf power source. However, atomic oxygen lines were found to be highly abundant. The presence of weak nitrogen lines indicated the presence of a small air leak to the plasma chamber.

Samples were carefully placed at the homogeneous portion of the plasma, in the SPI asher, which extends roughly from about 2 to 8 cm measured from the back of the asher chamber.⁴ A clean microscope glass slide was placed horizontally within the inner tube of the chamber so that it was supported at the shorter edges by the inner wall of the tube (see Fig. 2), and samples under investigation were placed horizontally on this glass slide. The flux of oxygen plasma was first calibrated by introducing four pieces of Kapton polyimide placed side by side along the glass slide (three samples of 1-cm² and one sample of 4-cm² area) in the asher, and ashing for various lengths of time and measuring the mass loss. It is known that Kapton adsorbs considerable moisture from the atmosphere.⁵ Therefore, Kapton samples were kept in a vacuum of about 10⁻⁵ Torr for more than two days before the ashing experiments were carried out, so that water molecules were desorbed from the Kapton surface. The results of Kapton mass loss versus ashing time are shown in Fig. 3. The linear least-square fits to the experimental data

TABLE I. Identification of plasma emission lines.

Wavelength (Å)	Identification (Tabulated wavelength) ^a
7772.4	O (7771.9)
6562.1	H (6562.7)
4358.6	N (4358.3)
4327.6	O (4327.5)
4089.7	O (4089.3)

^a See Ref. 24.

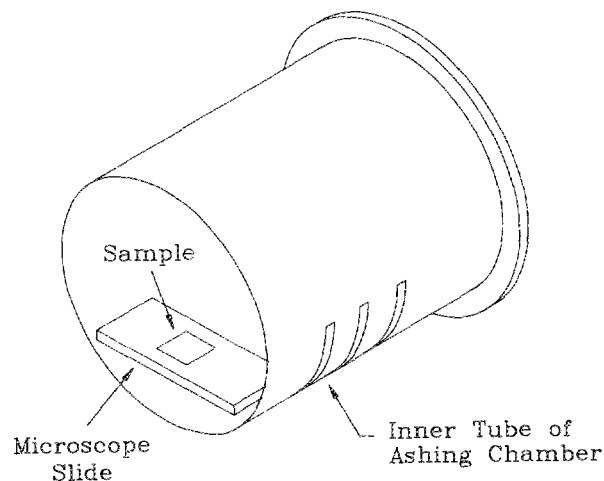


FIG. 2. Placement of samples and supporting glass slides in the Plasma Prep II asher.

are also shown in the same figure. Notice that there was very little plasma inhomogeneity (in terms of the amount of Kapton etched) along the transverse direction of the tube. The average Kapton mass-loss rate was determined to be 0.14 mg/cm²/h. Then, from the calibration curve of atomic oxygen fluence in space versus unit area Kapton mass-loss rate (Kapton was flown in a space shuttle bay and exposed to atomic oxygen in low-earth orbit), the *equivalent* atomic oxygen fluence rate in the asher was found to be approximately 4×10^{19} O atoms/cm²/h. It should be noticed that this is only a rough estimate giving a qualitative comparison between the atomic oxygen space environment and the oxidizing plasma environment in the asher, since the exact simulation of an atomic oxygen space environment in an asher is not possible.⁷

The temperature in the chamber was measured to be less than 70 °C by putting a series of special temperature-sensitive paints sandwiched between a common microscope glass slide and another very thin cover glass slide, inside the plasma for 30 min. The purpose of the thin cover slide was two-fold; first, to prevent the plasma from coming in direct contact with the paint and second, to conduct the heat to the paint as easily as possible without changing the plasma conditions.

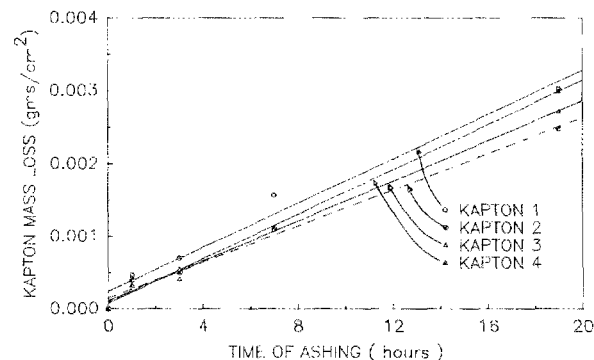


FIG. 3. Kapton mass loss vs ashing time in SPI Plasma Prep II asher.

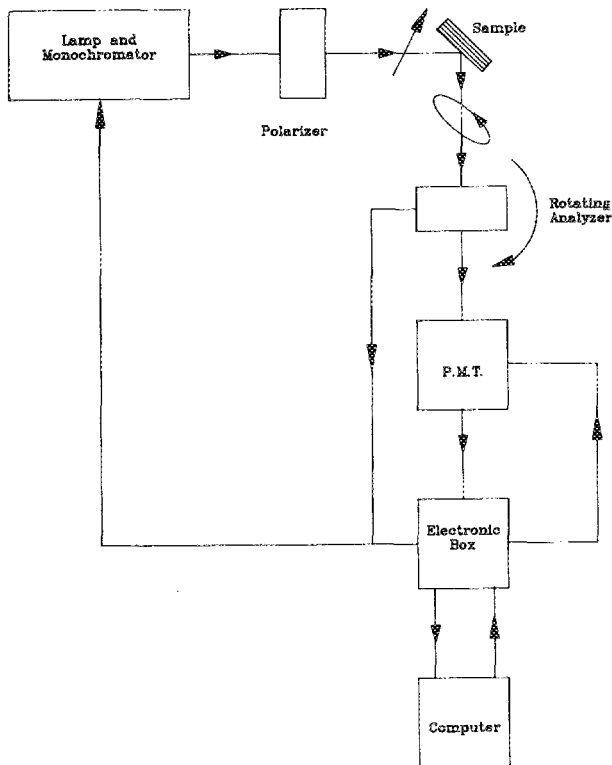


FIG. 4. Schematic diagram of the variable angle of incidence spectroscopic ellipsometer (VASE).

III. ELLIPSOMETRIC TECHNIQUE AND DATA ANALYSIS

Ellipsometry is known to be a nondestructive monolayer-sensitive experimental technique capable of taking *in situ* measurements in a wide range of environmental conditions. The success in the absolute determination of various optical and physical parameters largely depends on the degree of realistic modeling of the physical structure of the sample. In terms of finding the changes in the surface conditions of the sample, ellipsometry is a very reliable experimental method. The principles of ellipsometry stem from the principles of classical electrodynamics. A schematic diagram of the variable angle of incidence rotating analyzer spectroscopic ellipsometer is shown in Fig. 4. A linearly polarized plane parallel beam of collimated light is incident on the sample. (The beam diameter is typically about 1 mm.) The two component polarizations of light, one component in the plane of incidence and the other component perpendicular to the plane of incidence, upon reflection, undergo different phase retardations within the sample. As a result, one obtains an elliptically polarized reflected beam. By measuring the intensity of light passing through the rotating analyzer, and performing data analysis on the intensity versus analyzer azimuthal angle, one obtains the so-called ellipsometric parameters ψ and Δ . These parameters are defined in terms of the ratio of the complex Fresnel reflection coefficients r_p and r_s as follows:

$$r_p/r_s \equiv \tan \psi e^{i\Delta}.$$

For multilayer media, calculation of the Fresnel reflection coefficients from thicknesses and optical constants of individual layers becomes quite involved. The unknown parameters, such as the thickness and/or the optical constants for a particular layer are determined first by assuming some initial values for these parameters and then varying these parameters until the discrepancies between the calculated ψ and Δ values and the experimental ψ and Δ values are minimized. For this experiment, ψ and Δ data were taken for three different angles of incidence and over the wavelength range of 3000–8000 Å at 100-Å intervals. As a measure of the discrepancy between the experimental and calculated ψ and Δ values, one defines the mean-square-error function (MSE) by

$$\text{MSE} = \frac{1}{N} \sum_{i=1}^N [(\psi_{\text{exp}}^i - \psi_{\text{calc}}^i)^2 + (\Delta_{\text{exp}}^i - \Delta_{\text{calc}}^i)^2].$$

The goal of data analysis is to minimize this MSE by adjusting the unknown parameters for the various layers in the assumed model for the sample. To achieve that goal the Marquardt least-square algorithm¹⁷ has been used. From the data analysis, the sensitivity of the magnitude of the MSE function to the variation of a particular parameter is calculated. From that information, the 90% confidence limit to the value of this parameter is calculated. This 90% confidence limit is a measure of the error in the experimentally calculated parameter. (The error bars given in the plots of the experimental data denote this 90% confidence limit.) For a particular wavelength, better accuracy is obtained by increasing the number of angles of incidence for which ψ and Δ measurements are taken, since it imposes more constraints on the unknown parameters (optical constants for example) in the fitting procedure.

When there are two or more constituents in a certain layer, the optical constants of that layer are approximately obtained by applying the effective medium theory. In the analysis of silver oxide data, void and dense silver oxide were mixed together in the model, and the Bruggeman effective medium theory was applied to calculate the effective optical constants of that mixture layer. In this way, the optical constants of pure silver oxide were obtained from experiment.

IV. EXPERIMENTAL RESULTS

The samples were made by evaporating silver onto silicon(111) using resistive heating, followed by *e*-beam evaporating Al₂O₃, or SiO₂ on the top. The sample structures and their nominal thicknesses are given in Table II. The Al₂O₃/Ag/Si sample (A1), was cut into a piece about 1 × 1 cm², and exposed to an oxygen plasma in the SPI asher for 1,

TABLE II. Sample structures and nominal thicknesses.

Sample designation	Sample structure and Nominal thickness
A1	Al ₂ O ₃ (400 Å)/Ag(6000 Å)/Si
12A	SiO ₂ (800 Å)/Ag(400 Å)/Si
12B	SiO ₂ (800 Å)/Ag(400 Å)/Si

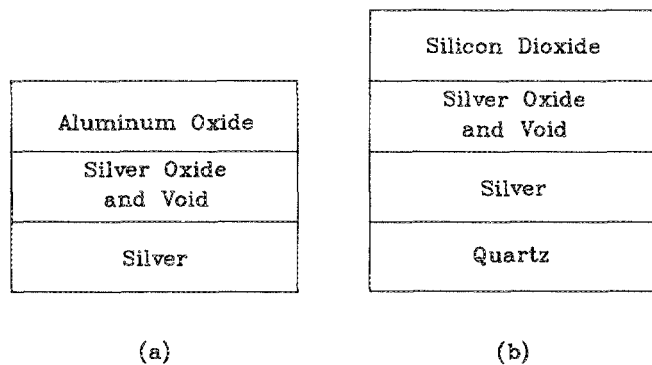


FIG. 5. (a) $\text{Al}_2\text{O}_3/\text{Ag-oxide}/\text{Ag}/\text{Si}$, (b) $\text{SiO}_2/\text{Ag-oxide and void}/\text{Ag}/\text{quartz}$: models used for ellipsometric data analysis of two kinds of samples shown in Table II.

3, 5.5, 9.5, and 13.5 h (cumulative). After each exposure, ellipsometric data were taken for three different angles of incidence: 60° , 65° , and 70° , and the resulting data for each exposure were analyzed assuming the three layer model shown in Fig. 5(a), where the top layer total thickness and optical constants were assumed to remain constant (with ashing). Since the silver layer was optically thick ($1 \mu\text{m}$), the effect of the silicon substrate was left out of the modeling scheme. The published silver oxide data²¹ did not result in a reasonable fit to the experimental ψ and Δ data, probably because the silver oxide sample prepared by Mayer and Muller was fundamentally different from the silver oxide data by VASE, a second experiment was carried out as described in the next paragraph.

An optically thick silver sample ($1 \mu\text{m}$ thick) was prepared and ellipsometrically measured almost immediately after taking it out of the deposition chamber. The resulting optical constants were compared with the published data for silver,²² and good agreement was found. This suggested that the silver sample was of good quality. The silver sample was next placed in the asher for three different cumulative times: 10, 30, and 60 s. After each exposure, ellipsometric data were taken for three different angles of incidence, as in the previous case, and over the same wavelength range. The 60-s ashed sample was so black that the ellipsometric data were not reliable since the photomultiplier tube did not have enough sensitivity to measure the low light level. As mentioned before, to extract the optical constants and thicknesses from the modeling and regression analysis of these ellipsometric data, good guesses of different parameters were needed. To start from good initial values of extinction coefficients (k) for the silver oxide layer, absorbance mea-

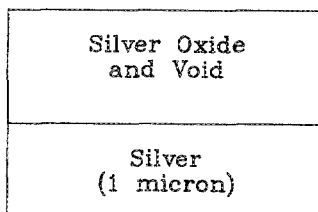


FIG. 6. Ag-oxide/Ag/Si: model used for the analysis of ellipsometric data on ashed Ag/Si samples.

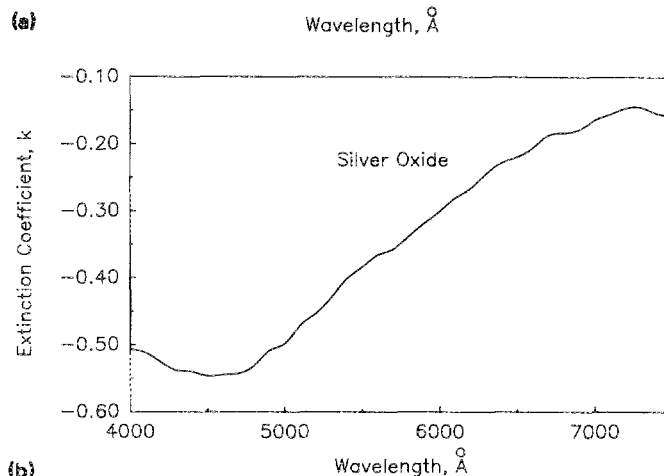
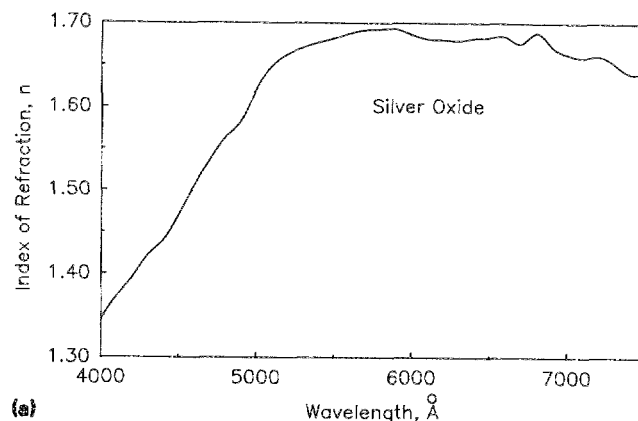


FIG. 7. (a) Refractive index, and (b) extinction coefficient for dense Ag-oxide, as measured by variable angle spectroscopic ellipsometry.

surements were performed on silver oxide as follows: a $500\text{-}\text{\AA}$ -thick silver layer was deposited on quartz, and ashed for 5 min. Absorbance measurements using a UV-VIS absorbance spectrometer were then made. Ashing for five more minutes did not change the absorbance data; an indication of the complete conversion of the silver layer to silver oxide. The absorbance is defined by the relationship: $A = \alpha d$, where $d = 500 \text{ \AA}$, and $\alpha = 4\pi k / \lambda$ (λ is the wavelength of light). Thus the measured absorbance provided good starting val-

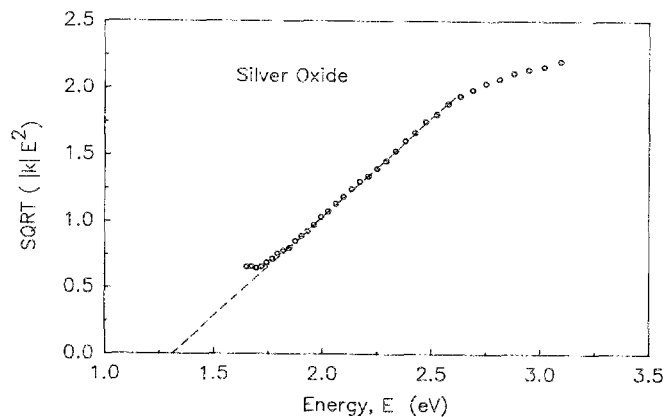


FIG. 8. Tauc plot for Ag-oxide.

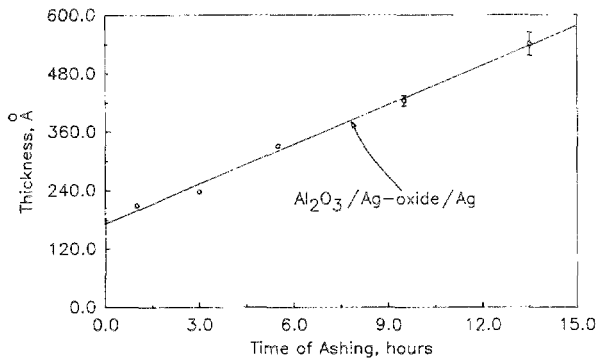


FIG. 9. Ag-oxide thickness vs ashing time as measured by VASE (sample A1).

ues for the evaluation of the extinction coefficients for the silver oxide layer. After a two layer model analysis (see Fig.6) of the ellipsometric data on the 10-s ashed sample, the optical constants for dense silver oxide were obtained. The results are shown in Fig. 7. By making a Tauc plot,²³ $E\sqrt{k}$ vs E , where E is the photon energy, the band gap for silver oxide was found to be 1.3 eV (see Fig. 8).

These silver oxide optical constants were then used to solve for the thickness of silver oxide and at the same time, the amount of void present in the silver oxide layer, produced as a result of ashing sample A1. The results of data analysis are shown in Figs. 9 and 10. From these figures, notice that the silver oxide becomes thicker with increased ashing, and at the same time it becomes more dense.

Experiments similar to those described above were carried out for the $\text{SiO}_2/\text{Ag}/\text{quartz}$ samples (12A and 12B). These two samples were cut from the same wafer and from adjacent locations. They were oxidized in the plasma asher under nominally the same conditions. The model used for analysis is shown in Fig. 5(b), and the silicon dioxide optical constants and layer thicknesses were assumed to remain constant. The results of the data analysis for various ashing times are plotted in Figs. 11 and 12. Figure 11 shows the loss of silver, which is subsequently converted to silver oxide. Figure 12 shows the total oxide thickness. During the first

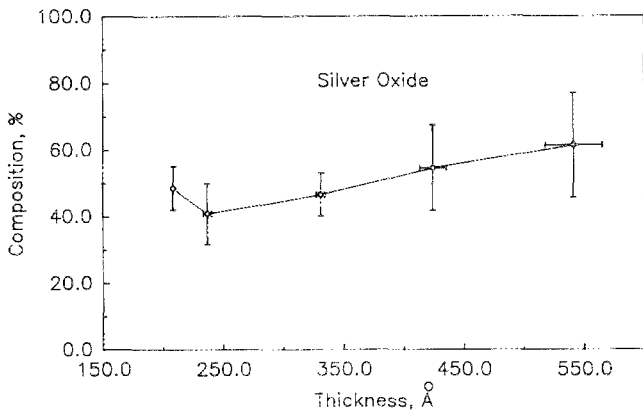


FIG. 10. Percentage of silver oxide vs silver oxide layer thickness as measured by VASE (sample A1).

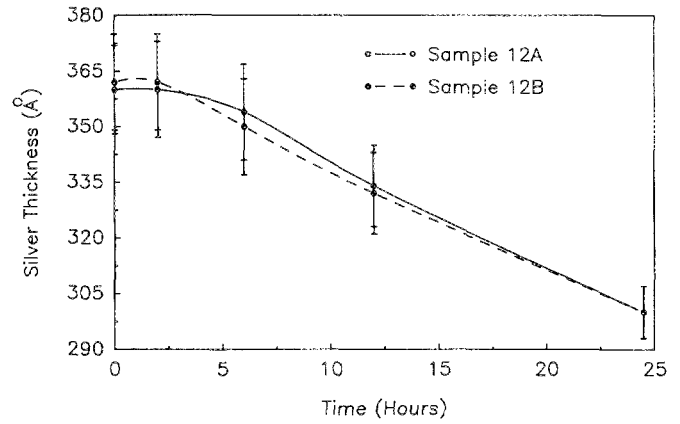


FIG. 11. Silver thickness as a function of ashing time for samples 12A and 12B.

two hours of ashing ellipsometric data did not change, indicating that oxygen still did not diffuse through the silicon dioxide layer. Analysis of VASE data show that, as with sample A1 data, a low-density silver oxide interfacial layer is formed under the initial oxide coating layer. If we assume that ashing has no effect on the silicon dioxide layer, then the silver oxide layer thickens by more than 100 Å. However, we believe that the Al_2O_3 and SiO_2 layers change properties somewhat, as a result of the atomic oxygen diffusion.

V. SUMMARY AND CONCLUSION

VASE measurements have been successfully applied to study the chemical conversion of a buried silver layer into silver oxide. It was found that atomic oxygen in the asher penetrated through the silicon dioxide or aluminum oxide protective coatings to convert the silver underneath to silver oxide. Increased ashing caused more silver to be converted to silver oxide. From three angles of incidence spectroscopic ellipsometry measurements on three silver oxide/silver samples, the silver oxide optical constants were calculated. The band gap of silver oxide was determined to be 1.3 eV. These optical constants are of general interest, as well as of interest for this specific application.

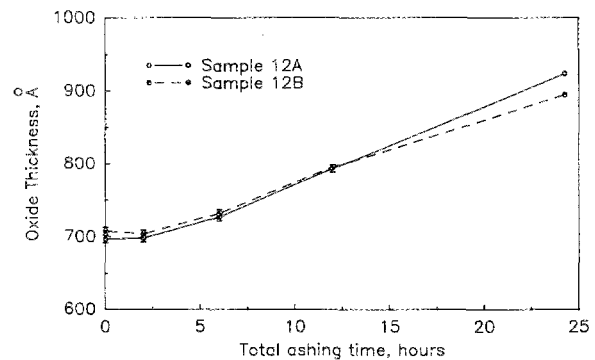


FIG. 12. Silver oxide thickness as a function of ashing time for samples 12A and 12B.

ACKNOWLEDGMENT

We would like to thank Dr. John Pouch of NASA Lewis for measurements of Auger profiles, and Kazem Memarzadeh for ellipsometric work early in the study.

¹B. A. Banks, M. J. Mirtich, S. K. Rutledge, and H. K. Nagra, in *Proceedings of the Eighteenth IEEE Photovoltaic Specialists Conference* (IEEE, New York, 1985), pp. 381–386.

²B. A. Banks, M. J. Mirtich, S. K. Rutledge, and D. M. Swec, "Sputtered Coatings for Protection of Spacecraft Polymers," NASA Report No. TM 83706, April, 1983.

³J. R. Hollahan and G. L. Carlson, *J. Appl. Polym. Sci.* **14**, 2499 (1970).

⁴B. A. Banks, M. J. Mirtich, S. K. Rutledge, D. M. Swec, and H. K. Nagra, "Ion Beam Sputter-Deposited Thin Film Coatings for Protection of Spacecraft Polymers in Low Earth Orbit," NASA Report No. TM 87051, January, 1985.

⁵S. K. Rutledge, B. Banks, F. DiFilippo, J. Brady, T. Dever, and D. Hotes, "An Evaluation of Candidate Oxidation Resistant Materials for Space Applications in LEO," NASA Report No. TM 100122, November, 1986.

⁶R. L. Parsons and D. A. Gulino, "Effect of an Oxygen Plasma on Uncoated Thin Aluminum Reflecting Films," NASA Report No. TM 89882, May, 1987.

⁷D. A. Gulino, R. A. Egger, and W. F. Bauhoizer, *J. Vac. Sci. Technol. A* **5**, 2737 (1987).

⁸J. B. Cross, E. H. Lan, and C. A. Smith, in *Proceedings of the 4th International Symposium on Spacecraft Materials in Space Environment*, September 6–9, 1988 (OMERA Centre d'études et de Recherches de Toulouse, Toulouse, France).

⁹D. A. Gulino, R. A. Egger, and W. F. Banholzer, *J. Vac. Sci. Technol. A* **5**, 2737 (1987).

¹⁰B. A. Banks, S. K. Rutledge, J. A. Brady, and J. E. Merrow, "Atomic

Oxygen Effects on Materials," NASA/SDIO Space Environmental Effects on Materials Workshop, June 28–30, 1988.

¹¹D. A. Gulino, "The Survivability of Large Space-Borne Reflectors Under Atomic Oxygen and Micrometeoroid Impact," NASA Report No. TM 88914, January, 1987.

¹²J. E. Klemberg-Sapieha, M. R. Wertheimer, and D. G. Zimeik, in *Proceedings of the 4th International Symposium on Spacecraft Materials in Space Environment*, September 6–9, 1988 (OMERA Centre d'études et de Recherches de Toulouse, Toulouse, France, 1988).

¹³B. A. Banks, M. J. Mirtich, S. K. Rutledge, D. M. Swec, and H. K. Nagra, "Ion Beam Sputter-Deposited Thin Film Coatings for Protection of Spacecraft Polymers in Low Earth Orbit," NASA Report No. TM 87051, January, 1985.

¹⁴R. M. A. Azzam and N. M. Bashara, *Ellipsometry and Polarized Light* (North-Holland, New York, 1977).

¹⁵P. G. Snyder, M. C. Rost, G. H. Bu-Abbud, J. A. Woollam, and S. A. Alterovitz, *J. Appl. Phys.* **60**, 3293 (1986).

¹⁶S. A. Alterovitz, J. A. Woollam, and P. G. Snyder, *Solid State Technol.* **31**, 99 (1988).

¹⁷G. H. Bu-Abbud, N. M. Bashara, and J. A. Woollam, *Thin Solid Films* **138**, 27 (1986).

¹⁸D. E. Aspnes and A. A. Studna, *Appl. Opt.* **14**, 220 (1975).

¹⁹J. A. Woollam, P. G. Snyder, and M. C. Rost, *Thin Solid Films* **166**, 317 (1988).

²⁰J. A. Woollam, P. G. Snyder, and M. C. Rost, *Mater. Res. Soc. Symp. Proc.* **93**, 203 (1987).

²¹S. T. Mayer and R. H. Muller, thesis, Lawrence Berkeley Laboratory, University of California, 1985.

²²E. D. Palik, Ed., *Handbook of Optical Constants of Solids* (Academic, New York, 1985).

²³N. F. Mott and E. A. Davis, Eds., *Electronic Processes in Non-Crystalline Materials* (Clarendon, Oxford, 1979).

²⁴G. R. Harrison, Ed., *MIT Wavelength Tables* (MIT Press, Cambridge, MA, 1969).